

# Well Test Analysis for Oil-Water Two-Phase Flow in Volume-Fractured Horizontal Wells

Jiaming Liu, Ruifei Wang

College of Petroleum Engineering, Xi'an Shiyou University, Xi'an, Shaanxi 710065, China

---

**Abstract:** Volumetric fracturing is crucial for developing low-permeability, tight reservoirs and unconventional formations, as its complex fracture networks greatly enhance reservoir flow capacity. However, oil-water two-phase flow in volumetrically fractured horizontal wells exhibits complex behaviors that traditional single-phase flow models fail to capture, reducing the accuracy of well test interpretations. To overcome this limitation, this study develops physical and mathematical models for oil-water two-phase flow by integrating two-phase flow theory with the fracture network characteristics of volumetrically fractured horizontal wells. Bottomhole pressure and pressure derivatives are obtained using Laplace transforms and the Stehfest numerical inversion method. Model validation against Eclipse numerical simulations and field well test data demonstrates high accuracy and reliability. Moreover, analysis of the well test curve identifies four characteristic flow regimes—fracture linear flow, fracture pseudo-radial flow, formation linear flow, and formation pseudo-radial flow—offering theoretical insights and technical support for understanding reservoir dynamics and optimizing development strategies.

**Keywords:** Volumetric fracturing, horizontal wells, oil-water two-phase flow, well test analysis, mathematical modeling.

---

## 1. Introduction

With the maturation of conventional oil and gas exploitation, the focus of production has shifted toward low-permeability, tight reservoirs and other unconventional formations [1, 2]. In these settings, volumetric fracturing has become a widely applied technique for horizontal well development, as it enhances fracture network complexity and significantly improves reservoir flow capacity [3-5]. Nevertheless, the complex fracture systems of fractured horizontal wells, coupled with the nonlinear behavior of two-phase oil-water flow, present considerable challenges for understanding reservoir flow mechanisms and conducting reliable well test analysis [6-8].

In particular, the coexistence of oil and water during development introduces additional complexity to well testing. Traditional single-phase flow models fail to capture the interactions between fluids in both fractures and the matrix, limiting the accuracy and reliability of test interpretation [9]. Thus, it is of theoretical and engineering significance to establish physical and mathematical models of oil–water two-phase flow specifically tailored to volumetrically fractured horizontal wells, and to investigate the characteristic responses of well test curves.

This thesis addresses well test analysis of oil-water two-phase flow in volumetrically fractured horizontal wells. The research scope includes: (1) constructing a physical model of oil-water two-phase flow based on fracture network characteristics; (2) developing the corresponding mathematical model using porous media flow theory; (3) validating and analyzing the model with field production data; and (4) identifying and interpreting well test curve features. The study aims to provide both a theoretical framework and practical methodologies for well test analysis, thereby offering guidance for the efficient development of fractured horizontal wells.

## 2. Well Test Analysis

In conventional fractured horizontal wells, artificial fracturing typically produces a single dominant fracture. By contrast, volumetrically fractured horizontal wells create complex fracture networks that markedly shorten the migration pathways of fluids from the matrix to the fractures, enhance the reservoir's effective permeability, and ultimately improve the development performance of shale oil reservoirs. In this chapter, a well-test mathematical model for oil-water two-phase flow in volumetrically fractured horizontal wells is established on the basis of two-phase flow theory and mathematical-physical methods. The model is solved using the Laplace transform in combination with the Stehfest numerical inversion algorithm. Building on this framework, the dynamic characteristics of well-test curves under oil–water two-phase flow are systematically examined, and a sensitivity analysis of pressure-response parameters is conducted to clarify the flow behavior of reservoir fluids within the formation.

### 2.1. Physical Model of Oil-Water Two-Phase Flow for Volumetrically Fractured Horizontal Wells

A volumetrically fractured horizontal well is assumed to be located at the center of a horizontal, homogeneous, isothermal reservoir of uniform thickness and infinite lateral extent, and to produce at a constant rate. The reservoir has impermeable top and bottom boundaries. Along the horizontal wellbore,  $n$  primary artificial fractures are uniformly distributed; these fractures intersect the wellbore perpendicularly and fully penetrate the formation. Each primary fracture is further intersected by  $2n_s$  secondary fractures, which are uniformly distributed and oriented perpendicular to the primary fracture. The permeability and width of the primary fractures are denoted as  $k_F$  and  $W_F$ , respectively, and those of the secondary fractures as  $k_f$  and  $W_f$ . Both primary and secondary fractures are modeled as vertical fractures with

finite conductivity, allowing pressure drop along the fracture direction.

The horizontal wellbore length is  $L_h$ , the half-length of a primary fracture is  $L_F$ , and the half-length of a secondary fracture is  $L_f$ . Reservoir fluids are considered slightly compressible and follow two-phase (oil-water) Darcy flow under isothermal conditions. Fluid flow inside fractures is one-dimensional along the fracture direction and is assumed to reach steady state. Fluids are produced from the matrix into both primary and secondary fractures; fluids in the secondary fractures flow only into the primary fractures, which then discharge into the wellbore. Fracture tips are treated as closed boundaries, and direct inflow from the reservoir or secondary fractures into the wellbore is neglected. The model is confined to two-dimensional flow and ignores gravity effects. A schematic diagram of the physical model is presented in Fig. 1.

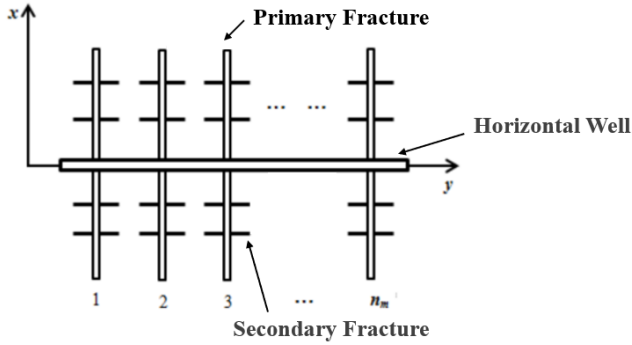


**Figure 1.** Schematic diagram of the physical model for oil-water two-phase flow in a volume-fractured horizontal well

$$\bar{p}_D = (1 - f_{w1}) \bar{q}_D \int_{y_{wD} - \Delta L_{FD}/2}^{y_{wD} + \Delta L_{FD}/2} k_0 \sqrt{(x_D - x_{wD})^2 + (y_D - \alpha)^2} \sqrt{(1 - f_{w1})u} d\alpha \quad (2)$$

Here,  $X_D$  and  $Y_D$  are the dimensionless coordinates of any point in the formation,  $X_{wD}$  and  $Y_{wD}$  are the coordinates of the center point of the primary fracture segment, and  $\Delta L_{FD}$  is

$$\bar{p}_{aD2} = (1 - f_{w1}) \bar{q}_D \int_{x_{wD} - \Delta L_{wD}/2}^{x_{wD} + \Delta L_{wD}/2} k_0 \sqrt{(x_D - \alpha)^2 + (y_{CD} - y_{wD})^2} \sqrt{(1 - f_{w1})u} d\alpha \quad (3)$$

the dimensionless length of the primary fracture segment. Using the same method, the secondary fractures are discretized and integrated to obtain the dimensionless bottom-hole pressure solution in the form of a line source.

### 2.2.2. Fracture Model

Based on the theory of oil-water two-phase seepage flow

$$\bar{p}_{FD}(x_D) - \bar{p}_{wD} = \frac{2\pi(1-f_{w2})}{c_{FD}} \int_0^{x_D} \int_0^\omega \bar{q}_{FD} d\alpha d\omega - \frac{2\pi q_{FD}(1-f_{w2})}{c_{FD}} x_D \quad (4)$$

and the point source function, a one-dimensional fracture system model for stable oil-water two-phase seepage flow is established. Using Laplace transform and integration methods, the pressure difference between any point in the primary fracture and the bottom-hole pressure in Laplace space is obtained as:

$$\bar{p}_{fD}(x_D) - \bar{p}_{wD} = \frac{2\pi(1-f_{w2})}{c_{FD}} \int_0^{x_D} \int_0^\omega \bar{q}_{fD} d\alpha d\omega - \frac{2\pi q_{fD}(1-f_{w2})}{c_{FD}} x_D \quad (5)$$

entire half-wing length of the primary fracture. The pressure difference between any point in the secondary fracture and the bottom-hole pressure in Laplace space is:

### 2.2.3. Model Discretization and Coupled Solution

The fractures are discretized, and a semi-analytical method

## 2.2. Mathematical Model of Oil-Water Two-Phase Flow for Volumetrically Fractured Horizontal Wells

To establish the mathematical model of oil-water two-phase flow for a volumetrically fractured horizontal well, a reservoir model and finite-conductivity vertical fracture models for the primary and secondary fractures are first constructed separately; these are then coupled and solved to obtain the dimensionless bottomhole pressure solution for the volumetrically fractured horizontal well.

### 2.2.1. Reservoir model

Based on the theory of oil-water two-phase seepage flow and the point source function, a reservoir model in an infinite formation is established, and the Laplace transform method is applied to solve it. The dimensionless point source solution of bottom-hole pressure under oil-water two-phase seepage flow conditions is thus obtained.

$$\bar{p}_D = (1 - f_{w1}) \bar{q}_D k_0 (r_D \sqrt{(1 - f_{w1})u}) \quad (1)$$

Here,  $f_{w1}$  represents the water cut in oil-water two-phase seepage flow. The volume-fractured horizontal well includes both primary and secondary fractures, both of which are regarded as vertical fractures with finite conductivity. Each primary fracture is discretized into several fracture segments, where the flow rate distribution may vary among segments but is assumed uniform within each segment. By integrating the primary fracture segments, the dimensionless bottom-hole pressure solution, treating the primary fracture segments as line sources, can be obtained.

is employed to solve the model. Each primary and secondary fracture is divided into multiple uniform-flow fracture segments. The Duhamel superposition principle is then applied to superimpose the pressure contributions of all fracture segments at the bottom hole. As shown in Fig. 2, a schematic diagram of the discretization of fractures in a volume-fractured horizontal well is provided.

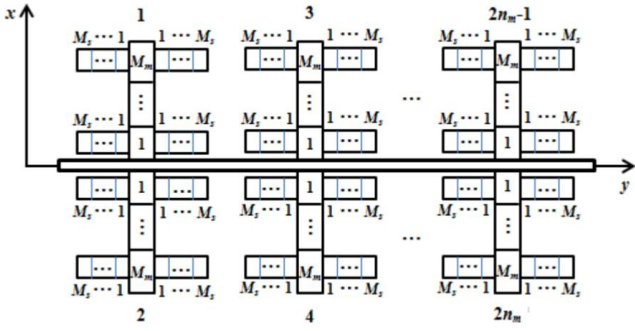


**Figure 2.** Schematic Diagram of Model Discretization for Volume-Fractured Horizontal Wells

#### Discretization of the Reservoir Model:

As shown in Fig. 2, assume the number of primary fractures

$$\bar{p}_{\alpha D1ij,lm} = (1-f_{w1})\bar{q}_{D,lm} \int_{y_{wD,lm}-\Delta L_{fD,lm}/2}^{y_{wD,lm}+\Delta L_{fD,lm}/2} k_0(\sqrt{(x_{D,ij}-x_{wD,lm})^2+(y_{D,ij}-\alpha)^2}\sqrt{(1-f_{w1})u})d\alpha \quad (6)$$

According to Equation 6, the pressure response generated by the discrete fracture element in the  $m$ -th segment of the  $l$ -

$$\bar{p}_{\alpha D2ij,lm} = (1-f_{w1})\bar{q}_{D,lm} \int_{y_{wD,lm}-\Delta L_{gD,lm}/2}^{y_{wD,lm}+\Delta L_{gD,lm}/2} k_0(\sqrt{(x_{D,ij}-\alpha)^2+(y_{D,ij}-y_{wD,lm})^2}\sqrt{(1-f_{w1})u})d\alpha \quad (7)$$

According to the Duhamel superposition principle, the pressure response at the discrete fracture element in the  $j$ -th

$$\bar{p}_{D,ij} = \sum_{l=1}^{2n_m} \sum_{m=1}^{M_m} \bar{p}_{\alpha D1ij,lm} + \sum_{l=1}^{2n_m \times 2n_s} \sum_{m=1}^{M_s} \bar{p}_{\alpha D2ij,lm} \quad (8)$$

#### Discretization of the Fracture Model:

The Fredholm integral equation is solved numerically using discretization methods. Each half-wing of the artificial

$$\bar{p}_{FD(xD)} - \bar{p}_{wD} = \frac{2\pi(1-f_{w2})}{C_{FD}} \left[ \frac{\Delta x_{Di}^2}{8} \bar{Q}_{FD,ij} + \sum_{N=1}^{j-1} \left( \frac{\Delta x_{Di}^2}{2} + (x_{D,ij} - N\Delta x_{Di}) \right) \bar{Q}_{FD,ij} - x_{D,ij} \sum_{j=1}^{Min} \bar{Q}_{FD,ij} \right] \quad (9)$$

Where  $i=1, 2, \dots, 2n_m$ ;  $j=1, 2, \dots, M_m$ ;  $\Delta x_{Di} = \frac{L_{FD}}{M_m}$ ,  $\Delta x_{Di}$

is the dimensionless length of the discrete fracture element of the  $ii$ -th primary fracture;  $x$  is the center point coordinate of the discrete fracture element at the  $jj$ -th segment of the  $ii$ -th primary fracture.  $\bar{Q}_{FD,ij}$  is the dimensionless flow rate at the  $jj$ -th segment of the  $ii$ -th primary fracture. At the intersection of the primary and secondary fractures, the flow rate at the  $jj$ -th segment of the  $ii$ -th primary fracture includes not only the flow rate of the primary fracture segment but also the flow rate from the secondary fractures intersecting with the

$$\bar{p}_{fD,im} - \bar{p}_{fD,ij} = \frac{2\pi(1-f_{w2})}{C_{FD}} \left[ \frac{\Delta x_{Di}^2}{8} \bar{q}_{FD,ij} + \sum_{N=1}^{m-1} \left( \frac{\Delta x_{Di}^2}{2} + (x_{D,im} - N\Delta x_{Di}) \right) \bar{q}_{FD,im} - x_{D,im} \sum_{m=1}^{ME} \bar{Q}_{FD,im} \right] \quad (11)$$

Where  $l=1, 2, \dots, n_s \times 2n_m$ ;  $j=1, 2, \dots, M_s$ ;  $\Delta x_{Dl} = \frac{L_{fD}}{M_s}$ ,  $x_{D,lm} = (i-1/2)\Delta x_{Dl}$ .

$\bar{p}_{fD,ij}$  is the dimensionless pressure at the  $jj$ -th segment of the  $ii$ -th secondary fracture;  $-\bar{q}_{fD,ij}$  is the dimensionless flow rate at the  $jj$ -th segment of the  $ii$ -th secondary fracture;  $\Delta x_{Di}$  is the dimensionless length of the discrete fracture element of the  $ii$ -th secondary fracture;  $\Delta x_{Dij}$  is the center point coordinate of the discrete fracture element at the  $jj$ -th segment of the  $ii$ -th secondary fracture.

#### Additional Equations:

Based on the conditions at the discrete fracture elements, where the pressure in the primary and secondary fractures

is  $n_m$ , and the number of secondary fractures on each primary fracture is  $n_s$ . Each half-wing of the primary fractures is uniformly divided into  $M_m$  segments, resulting in all primary fractures being discretized into  $n_s \times 2M_s \times 2n_m$  fracture elements. Each half-wing of the secondary fractures is uniformly divided into  $M_s$  segments, meaning all secondary fractures are discretized into  $n_s \times 2M_s \times 2n_m$  fracture elements. Assume the center point coordinates of the discrete fracture element in the  $mm$ -th segment of the  $ll$ -th fracture are  $(x_{wD}, l_m, y_{wD}, l_m)$ , and the center point coordinates of the discrete fracture element in the  $jj$ -th segment of the  $ii$ -th fracture are  $(x_{D,ij}, y_{D,ij})$ . The pressure response generated by the discrete fracture element in the  $mm$ -th segment of the  $ll$ -th primary fracture on the discrete fracture element in the  $jj$ -th segment of the  $ii$ -th fracture is:

th secondary fracture on the discrete fracture element in the  $j$ -th segment of the  $i$ -th fracture is:

segment of the  $i$ -th fracture, generated by all discrete fracture elements, is:

primary fractures is discretized into  $M_m$  discrete fracture elements, allowing the equation to be rewritten as:

primary fracture, as shown in Equation 9.

$$\bar{Q}_{FD,ij} = \begin{cases} \bar{q}_{FD,ij} + \frac{\sum q_{fDL} \cdot L_{fD}}{L_{FD}} \\ \bar{q}_{FD,ij} \end{cases} \quad (10)$$

Where  $\sum q_{fDL}$  represents the linear density flow rate of the secondary fracture segments intersecting with the primary fracture.

Each half-wing of the secondary fractures is discretized into  $M_s$  discrete fracture elements, allowing the equation to be rewritten as:

equals the reservoir pressure at the fracture face, and the flow rate at the fracture face equals the reservoir flow rate, the following equations are derived:

$$\begin{aligned} \bar{p}_{FD,ij} &= \bar{p}_{D,ij} \\ \bar{q}_{FD,ij} &= \bar{q}_{D,ij} \\ \bar{p}_{fD,ij} &= \bar{p}_{D,ij} \\ \bar{q}_{fD,ij} &= \bar{q}_{D,ij} \end{aligned} \quad (12)$$

According to the flow rate constraint condition, the normalized condition for fracture flow rate distribution is obtained:

$$\sum_{i=1}^{2n_m} \sum_{j=1}^{M_m} q_{FD,jj} \Delta x_{Dm} + \sum_{i=1}^{2n_m \times 2n_s} \sum_{j=1}^{M_s} q_{fd,ij} \Delta x_{Ds} = \frac{1}{u} \quad (13)$$

By combining Equation 6 and Equation 12, a reservoir model matrix of order  $2n_m \times M_m + 2n_m \times 2n_s \times M_s + 1$  and a fracture model matrix of the same order can be obtained. Coupling these two matrices and solving them numerically via MATLAB programming yields the dimensionless bottom-hole pressure value in Laplace space. The solution accounts for both wellbore storage effects and skin effects. Using the Stehfest numerical inversion algorithm, the curves of dimensionless bottom-hole pressure and its derivative in real space can be derived.

### 2.3. Case Study Validation and Analysis

To verify the accuracy and reliability of the proposed model, this study employs Eclipse numerical simulation software to establish a single-well numerical model for oil-water two-phase flow in a volume-fractured horizontal well. The dimensionless pressure and pressure derivative curves obtained from this numerical model are compared with those derived from the analytical model proposed in this study, plotted on the same log-log coordinate graph. The basic reservoir and fluid properties used in the modeling process include: Reservoir thickness: 10 m, Permeability: 0.13 mD, Porosity: 0.17; Fluid properties: water viscosity of 0.1 mPa·s, crude oil viscosity of 5 mPa·s; Production conditions: oil production rate of 30 m<sup>3</sup>/d, initial formation pressure of 20 MPa; Wellbore and fracture parameters: horizontal section length of 1000 m, 6 primary fractures (each with 4 secondary fractures), primary fracture half-length of 50 m, secondary fracture half-length of 10 m, primary fracture conductivity of 60 md·m, and secondary fracture conductivity of 30 md·m. Figure 3.3 demonstrates that the pressure and pressure derivative curves obtained from the analytical model for oil-water two-phase flow in volume-fractured horizontal wells proposed in this study show strong agreement with the Eclipse single-well numerical simulation results. To further validate the model's applicability, measured data from Well S1-1 are used for fitting analysis (see Fig. 3). Based on the established oil-water two-phase flow model for volume-fractured horizontal wells, repeated parameter adjustments and fitting tests confirm that the theoretical curves align well with the measured data. In conclusion, both the numerical simulation validation and the case study data fitting results indicate that the proposed model can accurately characterize the oil-water two-phase flow behavior in volume-fractured horizontal wells, effectively verifying its correctness and reliability.

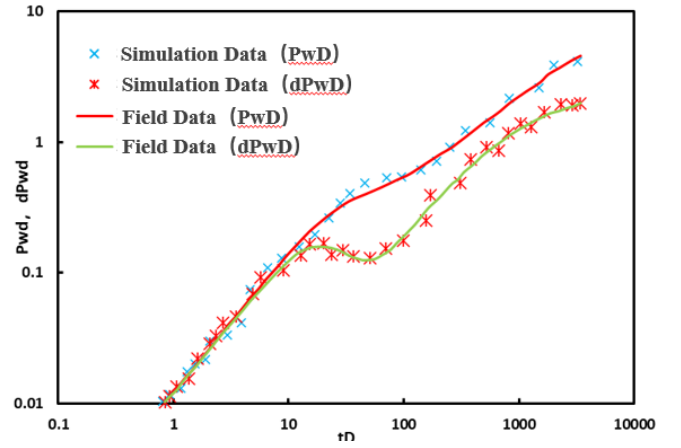


Figure 3. Example Validation of the Mathematical Model for Volume-Fractured Horizontal Wells

### 2.4. Analysis of Well Test Curve Characteristics

Based on the established well test model for oil-water two-phase flow in conventional fractured horizontal wells, a semi-analytical method combined with MATLAB programming was employed to calculate the dimensionless bottom-hole pressure and its derivative for volume-fractured horizontal wells. Subsequently, characteristic well test curves were plotted, accounting for changes in water cut within both the reservoir system and the fracture system. Figure 4 presents the characteristic well test curves for oil-water two-phase flow in fractured horizontal wells, where the model incorporates the time-dependent variation of water cut in both the reservoir and fracture systems. In the figure, PwD and dPwD represent the dimensionless bottom-hole pressure and its derivative, respectively, while tD denotes dimensionless time. Based on the characteristics of the well test curves, the well test response process for conventional fractured horizontal wells can be divided into four typical stages:

(1) Fracture Linear Flow Stage: In this stage, fluid primarily flows linearly perpendicular to the fracture faces, with each fracture acting independently without significant pressure interference. The characteristic feature is that the dimensionless pressure and pressure derivative curves appear as parallel straight lines.

(2) Fracture Pseudo-Radial Flow Stage: During this stage, the dimensionless pressure derivative curve exhibits a horizontal straight line. When the artificial fractures are short and widely spaced, pseudo-radial flow tends to develop around the fractures. As the pressure wave propagates toward the fracture tips and no interference between fractures occurs, the fluid streamlines around the fractures approximate a circular pattern, manifesting as pseudo-radial flow.

(3) Formation Linear Flow Stage: At this stage, the pressure wave has expanded to the regions between adjacent fractures, and pressure interference between fractures begins to occur. Fluid primarily flows linearly parallel to the artificial fracture faces.

(4) Formation Pseudo-Radial Flow Stage: As the pressure wave propagates further outward beyond the influence range of the fractured horizontal well, the fluid streamlines in the formation gradually form an approximately circular distribution around the horizontal well and artificial fractures,

exhibiting formation pseudo-radial flow.

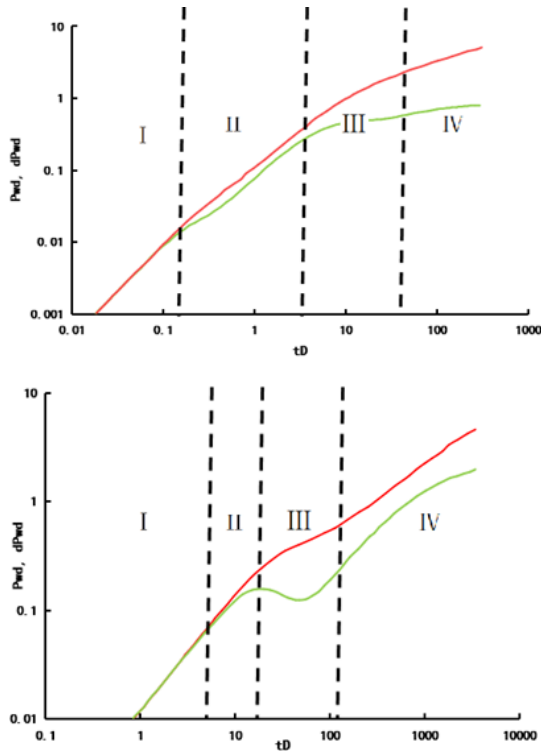


**Figure 4.** Characteristic Well Test Curves for Two-Phase Flow in Fractured Horizontal Wells in Shale Reservoirs

### 3. Conclusions

(1) Based on oil-water two-phase seepage theory and the characteristics of complex fracture networks in volume-fractured horizontal wells, this study developed physical and mathematical models for two-phase flow. Through model discretization and coupled solutions, analytical solutions for bottom-hole pressure and its derivative were derived. The model's accuracy and reliability in characterizing reservoir seepage behavior were validated, providing a theoretical basis for well test analysis and development optimization in complex reservoirs.

(2) Comparative analysis with Eclipse numerical simulations and actual well test data demonstrated that the proposed model accurately captures the dynamic characteristics of oil-water two-phase flow in volume-fractured horizontal wells. The agreement between dimensionless pressure and pressure derivative curves verified the model's accuracy and demonstrated its practical

applicability in oilfield development.

(3) The well test curves generated by the proposed model identified four characteristic stages of oil-water two-phase flow: fracture linear flow, fracture pseudo-radial flow, formation linear flow, and formation pseudo-radial flow. These stages reflect complex reservoir fluid flow behavior and provide insights into dynamic interactions between reservoir and fracture systems. Furthermore, they provide guidance for optimizing fractured horizontal well design parameters.

### References

- [1] Liu, J., Wang, R., Song, P., Li, Y., & Zheng, S. (2025). Quantitative Characterization and Flow Simulation of Micropore Structure in Clastic Gas Reservoirs Based on Micron CT Scanning. *ACS omega*, 10(20), 20686-20700.
- [2] Zhao, J., Wang, L., Wei, B., & Kadet, V. (2025). CO<sub>2</sub> utilization and geological storage in unconventional reservoirs after fracturing. *Engineering*.
- [3] Lei, Z., & Daihong, G. (2024). New Model for Predicting Production Capacity of Horizontal Well Volume Fracturing in Tight Reservoirs. *ACS omega*, 9(10), 11806-11819.
- [4] Xu, C., Guo, S., & Liang, H. (2023). Numerical study failure characteristics of natural fracture under induced stress. *Energy Reports*, 10, 4332-4341.
- [5] Jizhou, T. A. N. G., Xiaohua, W. A. N. G., Xianfei, D. U., & Bing, M. A. (2023). Optimization of integrated geological-engineering design of volume fracturing with fan-shaped well pattern. *Petroleum Exploration and Development*, 50(4), 971-978.
- [6] Zhang, Z., Hu, J., & Zhang, Y. (2025). A semi-analytical model for fractured horizontal wells production considering imbibition during shut-in periods. *Petroleum Science and Technology*, 43(15), 1891-1909.
- [7] Xiao, H., He, S., Chen, M., Liu, C., Zhang, Q., & Zhang, R. (2025). Two-Phase Production Performance of Multistage Fractured Horizontal Wells in Shale Gas Reservoir. *Processes*, 13(2), 563.
- [8] Chang, H., Dai, C., Ji, B., & Zhang, H. (2025). Data assimilation of multi-stage fractured horizontal well in unconventional oil and gas reservoir: Field case study. *Geoenery Science and Engineering*, 246, 213659.
- [9] Gu, Q., Liu, Z., Yang, H., Han, J., Sun, Z., & Liu, S. (2025). Gas-Water Two-Phase Seepage Model of Capillary Bundle Considering Pore Throat Structure and Analysis of Influencing Factors. *Langmuir*, 41(28), 18554-18568.